Relationship between the microstructure and rheology of micellar solutions formed by a triblock copolymer surfactant

Y. C. Liu
Department of Materials Science and Engineering, Massachusetts Institute of Technology, Cambridge, Massachusetts 02139

S. H. Chen
Department of Nuclear Engineering, Massachusetts Institute of Technology, Cambridge, Massachusetts 02139

J. S. Huang
Exxon Research and Engineering Company, Annandale, New Jersey 08801

(Received 16 February 1996)

We study the relationship between microstructure and rheology of spherical micelles formed by a triblock copolymer consisting of polyethylene oxide and polypropylene oxide in aqueous solutions. Small angle neutron scattering (SANS) is used to determine the self-association and hydration of the micelles at various polymer concentrations and temperatures. The intermicellar interaction can be described as a hard core repulsion with surface attraction. At elevated temperatures, the polymeric micelles exhibit a higher degree of association, dehydration, and surface adhesion. The low shear viscosity of the micellar solution is evaluated as a sum of the hydrodynamic contribution and a contribution from the interparticle interaction. The latter part is calculated based on the formula proposed by de Schepper, Smorenburg, and Cohen [Phys. Rev. Lett. **5,** 2178 (1993)]. We adopt Baxter's model of a hard sphere with an adhesive surface to evaluate the interparticle structure factor and find that the surface attraction effectively increases the viscosity at high volume fractions. To calculate the relative viscosity at low shear rate of the polymeric micellar solutions, we use the volume fractions and intermicellar interaction potentials extracted from SANS data analysis. We obtain excellent agreement between the calculated viscosity values and the experimental measurements. [S1063-651X(96)11708-6]

PACS number(s): 61.12.Ex, 61.25.Hq, 82.70.Dd, 83.70.Hq

I. INTRODUCTION

Polyethylene oxide containing block copolymers represent a class of polymers that associate spontaneously in aqueous solutions. The self-association is often characterized by sensitivity to temperature, concentration, and solvency [1]. In particular, a family of triblock copolymer surfactants composed of polyethylene oxide and polypropylene oxide (PEO-PPO-PEO) of various molecular weights and block lengths, under trade names of Pluronics (from BASF) or Poloxamers (from ICI) [2], has been extensively studied [3]. Various techniques have been used, including static and dynamic light scattering [4,5], small angle neutron scattering (SANS) [6], fluorescence [7], thermal analysis with differential scanning calorimetry [8], and diffusivity study with NMR [9]. Phase diagrams have been examined at various temperature and concentration regions and shown the variety of phases of triblock copolymers in aqueous solutions [6,10]. The phases include single-chained polymer coil, micelle, liquid crystal, and mixed phases. By altering the total molecular weight and the relative PEO to PPO ratio, aggregation and phase behaviors can be controlled systematically. Consequently, the triblock copolymers have widespread industrial applications in detergency, dispersion stabilization, foaming-defoaming, emulsification, gelation [2], and pharmaceutical usages such as drug solubilization and controlled release and bioprocessing [3,11].

The self-association of PEO-PPO-PEO can be understood from the hydrophobic effect [12], and is ultimately determined by the hydrophobicity and hydrophilicity of the building blocks and their interactions with the polar solvent (water) [1,13]. Both PEO and PPO blocks show hydrophilicity at low temperature and increased hydrophobicity at high temperature. PPO is more hydrophobic than PEO and tends to aggregate together to avoid contact with polar solvent molecules. At high temperature or concentration, the copolymer chains aggregate to form micelles with PPO blocks shielded by a layer of PEO blocks that are relatively compatible with solvent molecules. Due to the structural and chemical similarity of the two building blocks, micellization of the triblock copolymer tends to exhibit a gradual rather than an abrupt transition. Both critical micellization concentration (CMC) and critical micellization temperature (CMT) exist and depend strongly on the molecular weight and relative hydrophobe- hydrophile ratio of the polymer surfactant.

Previous researchers have focused attention mainly on two aspects of the polymeric micellar systems [3]. One aspect is on the properties related to micelle formation, such as CMC and CMT, and on the microstructure such as aggregation number, volume fraction, size and shape of micelle, and their dependency on surfactant molecular weight and compositions [4,6]. The other aspect is on the thermodynamics of micellization, based either on enthalpy and entropy extracted from experimental CMC and CMT data and differential scanning calorimetry measurements [7], or on Flory-Huggins types of solute-solvent and solute-solute interaction theories [14]. A mean field lattice model has been developed to de-

scribe the micelle formation and explain the experimental trend semiquantitatively [13].

One of the most important features of the triblock copolymer solution is its rheological behavior, which leads to numerous practical applications. For example, the copolymer surfactant can be used as viscosity modifier and gelation agent. Viscosity of the solution can be effectively monitored by controlling the polymer concentration, temperature, shear, and pressure. However, the rheological behaviors are the least understood in comparison with the structure and thermal properties of the solution. Brown *et al.* studied the viscoelasticity of a gel phase formed by Pluronic P85 (PEO_{25}-PPO_{40}-PEO_{25}) using oscillatory shear measurements at a fixed low frequency [5]. Pandya *et al.* studied the viscosities of Pluronic L64 (PEO_{13}-PPO_{30}-PEO_{13}) in water at temperature ranges from 25 to 55 °C and concentration ranges from 1.0 to 10.0 g dl^{-1} [15]. In the work of Pandya *et al.*, Huggins constants K' and hydration numbers were extracted from the viscosity data, based on phenomenological formulations applicable in a relatively dilute solution. The authors avoided higher concentration regions but indicated that the complication was associated with the strong intermicellar interactions. The formulations developed for the dilute solution cannot explicitly address the interaction among the solute particles. Studies of rheology largely rely on existing experimental data. No prediction can be reasonably made for solute concentrations beyond the measurements.

Our work aims at establishing a relationship between the microstructure and interaction of the solution and the rheology. We present a method to relate the microstructure and interaction with the low shear viscosity and viscoelasticity for spherical micelles formed by a PEO-PPO-PEO block copolymer surfactant in aqueous solutions.

II. MICROSTRUCTURE OF POLYMERIC MICELLES

The triblock copolymer surfactant we study is Pluronic P84 from BASF. It contains 40 wt % of polyethylene oxide and 60 wt % of polypropylene oxide. Its corresponding chemical formula is PEO_{19}-PPO_{43}-PEO_{19}. This surfactant has total molecular weight of 4200 and molecular volume of 6920 $Å^3$. Micellar solutions were made with Pluronic P84 dissolved in deuterated water. Pluronic P84 polymer was used as received without further purification. Deuterated water was purchased from Cambridge Isotope Company. The cloud point of the solutions is 75 °C.

Micellization occurs above CMC and (CMT). Micellization has no sharp boundary but a rather broad coexistence region of large aggregates and single chained polymers. Dynamic light scattering shows that Pluronic micellar solution exhibits significant polydispersity at low temperature, and monodispersity at high temperature [4]. Batch-to-batch variations of the surfactant supplies with composition heterogeneities, such as diblock copolymer impurities, considerably affect micelle formation and surface tension, but have little effect on the micellar structure and intermicellar interaction. We focus on the microstructure and interaction of micelles and ignore the impurities and heterogeneity. The concentration and temperature ranges are selected within the micellar phase.

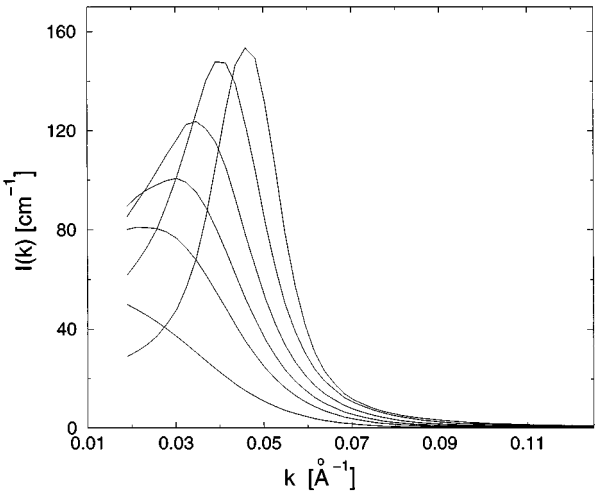

FIG. 1. SANS intensity distribution functions $I(k)$ for micellar solutions at polymer concentrations of 2.6, 6.1, 8.8, 12.5, 17.9, and 22.9 % at $T=55$ °C. Solutions at higher polymer concentrations have peaks at larger k_{max} values.

The size of the polymeric micelles formed by Pluronic P84 is about 10 nm. Detailed information about the micellar structure and interaction requires a probe having a wavelength comparable with the particle dimension. Small angle neutron scattering with a neutron wavelength in the range 5–10 Å is an appropriate and powerful tool. SANS measurements are made using a high contrast solvent D_2O against the hydrogenated block copolymer. It is assumed that no isotope effects are present with the microstructure of micelles.

SANS experiments were performed at the Brookhaven National Laboratory and the National Institute of Standards and Technology. The polymer solution samples were contained in 1-mm quartz cells. The neutron wavelength used was 7 Å. A series of polymer concentrations ranging from 2.6 to 23 wt % was studied at temperatures from 30 to 60 °C.

Figure 1 illustrates a typical series of SANS intensity distribution functions $I(k)$ (k is the magnitude of scattering wave vector) for different polymer concentrations at temperature $T=55$ °C. SANS intensity distribution functions indicate that the spatial correlations of micelles are liquidlike. Mortensen and co-workers used the hard sphere model to analyze SANS data of similar micellar solutions [6]. In their treatment, the hard sphere diameter for the structure factor, the radius for the spherical form factor, and the volume fraction were used as the independent fitting parameters. The scattering lengths' densities were approximately known. Although crude, the hard sphere model was successful in describing the characteristics of the polymeric micellar system.

The association of copolymer surfactant molecules is quite obvious from the increase of the scattering intensity with temperature. Figure 2 shows SANS intensity distribution $I(k)$ for a 12.5 wt % solution as temperature ranges from 21 to 55 °C. At the lowest temperature (21 °C), there is hardly any association. As the temperature increases, aggregates form and grow bigger, corresponding to higher peak intensities and peak positions k_{max} at smaller k.

The microstructure of the pluronic micelles has been in-

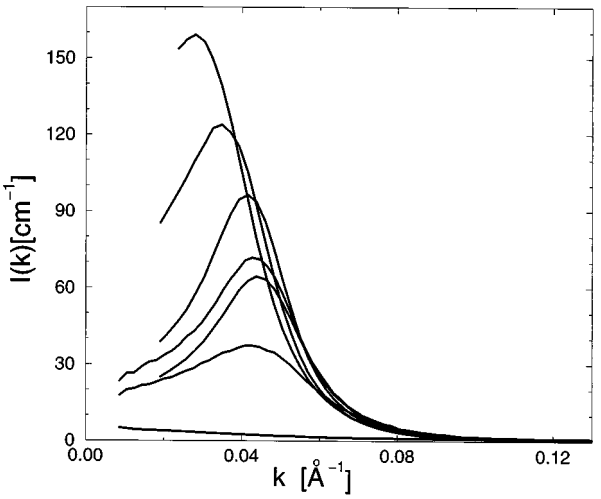

FIG. 2. SANS intensity distribution of 12.5 % micellar solution at 21, 30, 35, 40, 45, 55, and 60 °C. Higher peak amplitude corresponds to higher temperature.

vestigated by many researchers [1,4–6]. It is described as a sphere or an ellipsoid with a hydrophobic core and a hydrated corona. The core is composed of PPO segments, and the corona accommodates PEO segments and solvent molecules. The degree of association is described by the mean aggregation number, which is related to the radius of the hydrophobic core under the compact packing conditions. The degree of hydration is determined by the volume occupied by the solvent molecules in the corona, which is the difference between the micellar volume and the dry surfactant volume. The volume fraction of the micelles is determined by the number density of the micelles and the hydrated volume of each micelle.

Careful analysis of $I(k)$ can yield accurate information about the detailed microstructure of a micelle. The coherent scattering intensity from micelles in solution is written as

$$I(k)=cN\left[\sum_i b_i-\rho_s V_M\right]^2 P(k)S(k), \tag{1}$$

where $P(k)$ is the normalized particle form factor, $S(k)$ the interparticle structure factor, c the molar concentration of the polymeric surfactant, $\Sigma_i b_i$ the sum of the scattering lengths of all atoms in a surfactant molecule, V_M the volume of the surfactant, and ρ_s the scattering length density of the solvent. To account for the aggregation of the central block of the polymer and solvation, a two-shell model is adopted for evaluation of the form factor $P(k)$. The two-shell model has been successfully used in SANS data analysis of ionic micelles formed by sodium dodecyl sulfate [16].

$$P(k)=\left[\xi\frac{3j_1(ka)}{ka}+(1-\xi)\frac{3j_1(kb)}{kb}\right]^2, \tag{2}$$

where $j_1(k)$ is the spherical Bessel function of order one. The parameters a and b are the radius of the inner core and the outer corona. The dimensionless factor ξ describes the neutron scattering length distributions in the core and the corona.

$$\xi=\frac{v_{\mathrm{PPO}}(\rho_{\mathrm{core}}-\rho_{\mathrm{corona}})}{\Sigma_i b_i-\rho_s V_M}, \tag{3}$$

where ρ_{core} and ρ_{corona} are the scattering length densities of the micellar core and corona. The micellar core is assumed to be composed of densely packed PPO blocks.

$$\rho_{\mathrm{core}}=\frac{b_{\mathrm{PPO}}}{v_{\mathrm{PPO}}}. \tag{4}$$

The corona of the micelle contains PEO blocks and solvent molecules.

$$\rho_{\mathrm{corona}}=\frac{b_{\mathrm{PEO}}+Hb_{\mathrm{D_2O}}}{v_{\mathrm{PEO}}+Hv_{\mathrm{D_2O}}}, \tag{5}$$

where b_{PPO}, b_{PEO} and $b_{\mathrm{D_2O}}$ are scattering lengths of PPO block, two PEO blocks in the triblock copolymer molecule, and that of the solvent. $v_{\mathrm{D_2O}}$ is the molecular volume of D_2O solvent. v_{PPO} and v_{PEO} are the total volumes of PPO block and PEO blocks in a surfactant molecule. The hydration number H, defined as the average number of solvent molecules per copolymer chain, is determined by the volume occupied by water molecules in the outer corona.

$$H=\frac{(4\pi/3N)(b^3-a^3)-v_{\mathrm{PEO}}}{v_{\mathrm{D_2O}}}, \tag{6}$$

where the aggregation number N is related to the core volume by

$$N=\frac{4\pi/3a^3}{v_{\mathrm{PPO}}}. \tag{7}$$

The molecular volumes and scattering lengths of the constituting polymer segments and the solvent are listed in Table I. The total volumes and scattering lengths can be calculated

TABLE I. Molecular volumes and scattering lengths of the Pluronic P84 triblock copolymer surfactant and the solvent.

	Chemical formula	Molecular weight	Molecular volume (Å^3)	Scattering length Σb_i (10^{-5} Å)
EO	—$(CH_2)_2O$—	44	72.4	4.14
PO	—$(CH_2)_3O$—	58	95.4	3.31
P84	$PEO_{19}PPO_{43}PEO_{19}$	4200	6920	302.1
Solvent	D_2O	20	30.3	19.153

according to the chemical formula PEO_{19}-PPO_{43}-PEO_{19} for this copolymer surfactant. Given the aggregation number and the hydration number, the microstructure of a micelle can be determined.

The information about the microstructure is sufficient for a dilute suspension, for which the interactions among micelles are negligible. Micellar interaction and distribution must be taken into account for higher concentrations through the evaluation of the interparticle structure factor $S(k)$.

A hard sphere model with an adhesive surface is introduced in order to describe the attractive intermicellar interaction. We model the hard sphere with an adhesive surface in terms of the Baxter potential. The pairwise interparticle interaction potential is written as [17]

$$\frac{\phi(r)}{k_B T}=\begin{cases}+\infty & \text{for} \quad 0<r<R' \\ \Omega & \text{for} \quad R'<r<R \\ 0 & \text{for} \quad R<r,\end{cases} \tag{8}$$

where k_B is Boltzmann's constant and T absolute temperature. Baxter expressed the attractive potential Ω as

$$\Omega=\ln\left(12\tau\frac{R-R'}{R}\right). \tag{9}$$

This way the second virial coefficient of the system has a simple expression in terms of the parameter $1/\tau$. For the evaluation of viscosity, it is more appropriate to use the surface potential Ω.

Baxter used the Percus-Yevick approximation to calculate the structure factor to first order in the surface layer thickness. Define the fractional surface thickness $\epsilon\equiv(R-R')/R$ as being small but a finite number. The Ornstein-Zernike equation is solved under the conditions

$$H(r)=rh(r)=\begin{cases}-r & \text{for} \quad 0<r<R' \\ \dfrac{\lambda R^2}{12(R-R')} & \text{for} \quad R'<r<R\end{cases} \tag{10}$$

and

$$c(r)=0, \quad r>R, \tag{11}$$

where λ is determined by a solution of a quadratic equation involving the volume fractions ϕ and τ. The total correlation function $h(r)$ in the core is given by the varial expansion method. Baxter gave an analytical solution of the direct correlation function $c(r)$ inside the core as an explicit function of τ and ϵ, besides the volume fraction ϕ [17]. Define the following parameters at a given ϕ:

$$\begin{aligned}\Gamma&=\frac{\phi(1+\phi/2)}{3(1-\phi)^2},\\ \Delta&=\tau+\phi/(1-\phi),\\ \lambda&=\frac{6(\Delta-\sqrt{\Delta^2-\Gamma})}{\phi},\\ \mu&=\lambda\phi/(1-\phi),\end{aligned} \tag{12}$$

$$\begin{aligned}\alpha&=\frac{(1+2\phi-\mu)^2}{(1-\phi)^4},\\ \beta&=-\frac{3\phi(2+\phi)^2-2\mu(1+7\phi+\phi^2)+\mu^2(2+\phi)}{2(1-\phi)^4}.\end{aligned}$$

The dimensionless parameter $Q\equiv kR$ is defined as the product of the magnitude of the wave vector transfer k and the particle diameter R. The structure factor $S(Q)$ can be evaluated from the Fourier transform of the direct correlation function $c(Q)$, which contains a part from the hard core (HC) and an excess contribution due to the adhesive surface:

$$\frac{1}{S(Q)}-1=-4\pi\rho[c^{\mathrm{HC}}(Q)+c^{\mathrm{ex}}(Q)], \tag{13}$$

where ρ is the number density of the particles, and can be related to the volume fraction by $\phi=\pi/6\rho R^3$. Note that R corresponds to the minimum intermicellar distance and equals the diameter of the particle. More explicitly, the structure factor can be written in terms of the parameters defined above as

$$\begin{aligned}\frac{1}{S(Q)}-1=&24\phi\left[\alpha f_2(Q)+\beta f_3(Q)+\frac{1}{2}\phi\alpha f_5(Q)\right]\\ &+4\phi^2\lambda^2\epsilon^2\left[f_2(\epsilon Q)-\frac{1}{2}f_3(\epsilon Q)\right]\\ &+2\phi^2\lambda^2[f_1(Q)-\epsilon^2 f_1(\epsilon Q)]\\ &-\frac{2\phi\lambda}{\epsilon}[f_1(Q)-(1-\epsilon)^2 f_1((1-\epsilon)Q)]\\ &-24\phi[f_2(Q)-(1-\epsilon)^3 f_2((1-\epsilon)Q)].\end{aligned} \tag{14}$$

The functions $f_n(x)$ are defined as

$$\begin{aligned}f_1(x)&=\frac{1-\cos x}{x^2},\\ f_2(x)&=\frac{\sin x-x\cos x}{x^3},\\ f_3(x)&=\frac{2x\sin x-(x^2-2)\cos x-2}{x^4},\\ f_5(x)&=\frac{(4x^3-24x)\sin x-(x^4-12x^2+24)\cos x+24}{x^6}.\end{aligned} \tag{15}$$

The structure factor $S(Q)$ for hard spheres with adhesive surfaces is an explicit function of three parameters: the volume fraction ϕ, the surface adhesion potential Ω, and the fractional surface layer thickness ϵ.

Figure 3 illustrates $S(Q)$ at a constant volume fraction $\phi=0.3$ for a hard sphere system and adhesive hard sphere systems with $\Omega=-1$ and -2, where the fractional surface thickness is fixed at 0.01. The structure factors for hard spheres with different surface adhesive potentials are obvi-

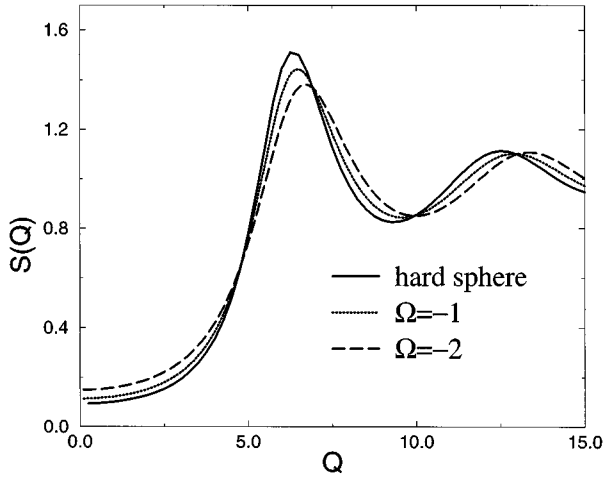

FIG. 3. Structure factor $S(Q)$ at volume fraction 0.3 and fixed surface thickness $\epsilon=0.01$ with various surface adhesive potentials Ω in contrast with the hard sphere model. Solid line is for hard sphere system. Dotted and dashed lines are for Ω of -1 and -2, respectively.

ously distinguishable. Meanwhile, the structure factor for the systems with the same surface potential and different layer thickness is also demonstrated. Figure 4 shows $S(Q)$ with a fixed surface potential $\Omega=-1$ but surface layer thickness ϵ ranging from 0.001 to 0.05. The structure factor is equally sensitive to the surface thickness as well as to the depth of the attractive potential.

The structure factor for an adhesive hard sphere system depends on both Ω and ϵ. However, it can be shown that $S(Q)$ is determined only by the parameter τ when ϵ is taken as infinitesimal. Fig. 5 shows the structure factors at $\phi=0.2$ for three different sets of (Ω, ϵ) with the same τ value ($\tau=3.066$). These three configurations are $(-2.609, 0.002)$, $(-1.0, 0.01)$, and $(0.0986, 0.03)$. In the upper graph, structure factors given by these three sets are hardly distinguishable at the small Q region. On the other hand, there are noticeable discrepancies at the large Q region. These discrepancies, as shown in the next section, result in drastically different rheological properties.

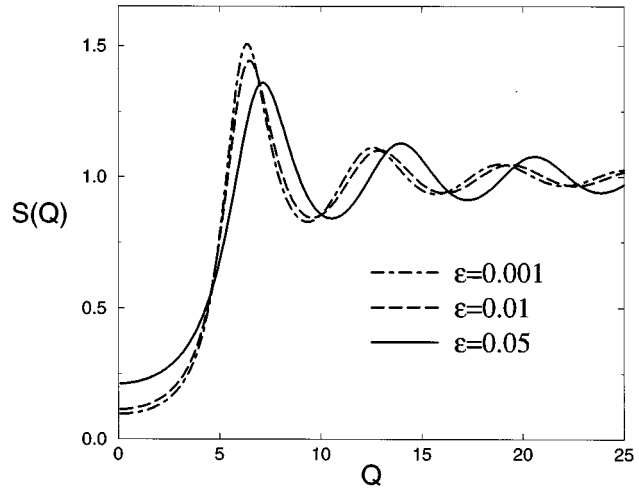

FIG. 4. Structure factor $S(Q)$ at volume fraction 0.3 and fixed potential $\Omega=-1$ with various surface thickness ϵ values. Solid, dashed, and dot-dashed lines are for ϵ of 0.05, 0.01, and 0.001, respectively.

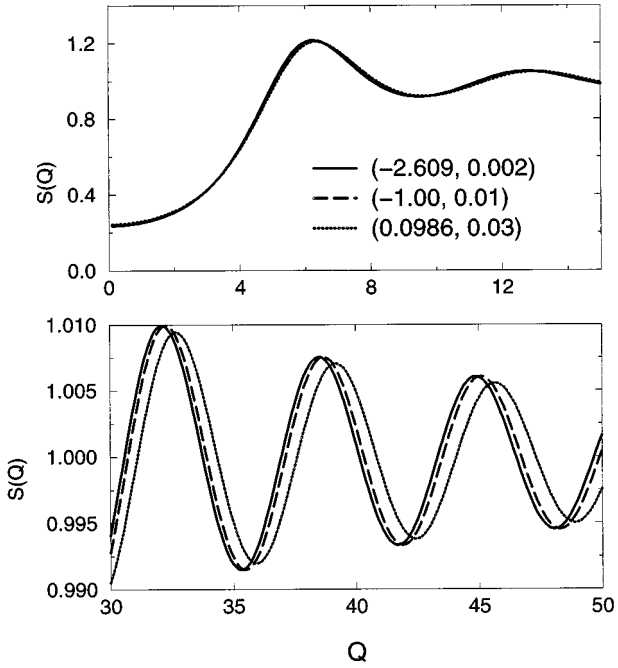

FIG. 5. Structure factor $S(Q)$ at volume fraction 0.2 and fixed $\tau=3.066$ from different configurations of Ω and ϵ. Solid, dashed, and dotted lines are for (Ω, ϵ) sets of $(-2.609, 0.002)$, $(-1.0, 0.01)$, and $(0.0986, 0.03)$, respectively. The upper and lower graphs indicate small Q (lower than 15) and large Q (higher than 30) behaviors, respectively.

The scattering intensity $I(Q)$ is proportional to the product of the interparticle structure factor $S(Q)$ and the intraparticle structure factor $P(Q)$. For Q larger than 15, the shape of $I(Q)$ is essentially suppressed by the fast decreasing $P(Q)$ since $S(Q)$ approaches unity. In a typical small angle neutron or x-ray scattering experiment, the structure factor $S(Q)$ can be considered to depend on the parameter τ only. The exact set of attractive potential and surface thickness simply cannot be resolved as far as the experimental resolution is concerned. This explains why Ku *et al.* successfully analyzed SANS data of a water-in-oil droplet microemulsion by using a sticky sphere model with τ as the only parameter [18]. Using two parameters Ω and ϵ is unlikely to obtain a unique set of fitting parameters.

To reduce the number of free parameters in SANS data analysis, a reasonable value for ϵ may be assigned. The diameter of the polymeric micelles is of the order of 100 Å, and presumably the sticky surface is of molecular dimension. We take $\epsilon=0.01$ for simplicity and use surface potential Ω as a free parameter throughout the procedure of SANS data analysis.

The microstructure and interaction of Pluronic P84 polymeric micelles can be obtained by fitting SANS data into an absolute intensity scale. We use three independent fitting parameters, the radius of inner core a, the radius of outer corona b, and the attractive potential Ω. Aggregation number and hydration number are calculated according to Eqs. (6)

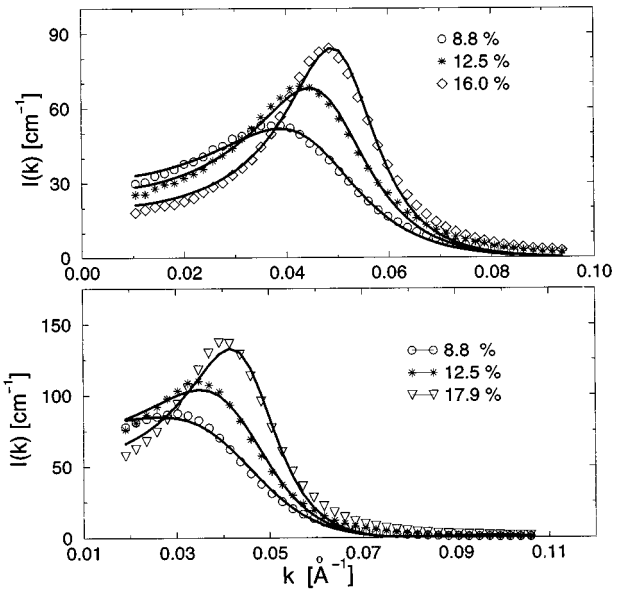

FIG. 6. SANS data and fits for P84 solutions at 40 °C (upper graph) and 55 °C (lower graph) in absolute intensity scales. Symbols are SANS data and solids lines are fits.

and (7) and further used to calculate the volume of a micelle. The number density of the micelles is equal to the number density of surfactant molecules divided by the mean aggregation number N. The volume fraction is given by the volume of a micelle and the number density of micelles. Thus the microstructure of the micelle is uniquely determined once the three fitting parameters are known.

SANS intensity distribution functions of Pluronic P84 are analyzed for five temperatures, 35, 40, 45, 55, and 60 °C. A Fortran code based on a gradient searching nonlinear least square fitting method is written and used to fit SANS data into absolute intensities. Fig. 6 shows some SANS data and fits at moderate concentrations at 40 and 55 °C. The quality of fitting is reasonably good for all the samples from 2.6 to 23 wt % at 35, 40, 45, and 55 °C. SANS fits at large k are poor due to the oversimplified particle form factor. The polymer segment distribution inside the hydrated corona of a micelle is more likely to vary with r rather than be a constant with a sharp boundary as described by the two-shell model. Furthermore, the two-shell sphere model is not valid for 60 °C because the shape of the micelle deviates from sphericity significantly.

Important parameters on the microstructure of the micelles are listed in Table II. The aggregation number and core radius can be determined within an accuracy of 2%, and other parameters of 5–10 %. The aggregation number of the micelle remains the same at different surfactant concentrations, but is very sensitive to temperature. As temperature increases from 35 to 55 °C, aggregation number increases from 63 to 105. The micellar core grows from 39.6 to 46.4 Å , but hydration decreases with temperature. The outer corona radius remains more or less the same (increased by a maximum 10%) in all the cases . This agrees with the results of many similar micellar solutions studied by other researchers [3]. It is also found that at a given temperature, the ratio of volume fraction of micelles to the volume of dry surfactant molecules is a constant, and furthermore the attractive potential is also a constant. This leads one to conclude that, in contrast with a typical ionic micellar solution, the microstructure of the micelles formed by the triblock copolymer of PEO and PPO is determined by temperature, and independent of the polymer concentration.

From the surface adhesion parameters, it is clear that the micelles grow and become stickier at elevated temperatures. The surface attractive potentials Ω turn out to be -0.51 at 35 °C, but -1.33 at 55 °C.

The microscopic parameters extracted from our SANS data analysis scheme are crucial quantities that determine the viscosity. It is remarkable that the important parameters can be obtained based on such a simple structural model. The quality of data fitting can be improved by taking into account the resolution factor (desmearing) and by more careful modeling of micellar microstructure. To correct the particle form factor $P(Q)$, modification can be made through taking into account the micellar size polydispersity, slight deviation from spherical shape, and diffusive density profile of the polymer chains. In practice it is difficult to distinguish the three effects by the scattering experiments. However, significant shape change occurs at high temperature, and chain conformation and distribution profile have little to do with the degree of hydration. In this paper we do not intend to elaborate on the more detailed microstructure as long as the overall volume fraction and interaction potential can be obtained with sufficient accuracy. The polymer chain distribution and shape effects will be discussed in future work.

III. RHEOLOGY OF HARD SPHERES WITH ADHESIVE SURFACES

The viscosity of colloidal dispersions in the limit of low volume fraction is described by Einstein's theory on hydrodynamic interaction between hard spheres [19]. Relative vis-

TABLE II. Parameters of microstructure and interaction of polymeric micelles extracted from SANS experiments.

Temperature (°C)	Aggregation N	Hydration H	Core radius (Å)	Diameter (Å)	Potential Ω	Stickiness $(\frac{1}{\tau}) \equiv 12\epsilon \exp(-\Omega)$
35	63	290	39.6	121	-0.51	0.199
40	68	250	40.2	125	-0.87	0.286
45	77	220	42.5	130	-1.17	0.387
55	105	160	46.4	133	-1.33	0.454

cosity η_r, defined as the ratio of the solution viscosity η to the solvent viscosity η_0, is related the volume fraction ϕ by

$$\eta_r = 1 + 2.5\phi. \tag{16}$$

At high volume fractions, the linear relationship is insufficient. It is common to adopt an empirical approach by expanding the relative viscosity to higher orders of volume fraction:

$$\eta_r = 1 + 2.5\phi + a_2\phi^2 + a_3\phi^3 + \cdots. \tag{17}$$

The polynomial coefficients obtained by different authors usually have different values, even in the simplest case of a hard sphere system. These coefficients are found to depend on shear, frequency, and even volume fraction ϕ. In the low shear limit, Batchelor obtained $a_2 = 6.2$ for hard spheres [21]. Phillips, Brady, and Bossis calculated $a_2 = 5.07$ [22]. de Kruif *et al.* calculated the range for the coefficients and found that $a_2 = 4 \pm 2$ and $a_3 = 42 \pm 10$ for the low shear limit while $a_3 = 25 \pm 7$ for the high shear limit [20]. Brady showed that the a_2 from Brownian contribution is proportional to the pair correlation function at contact [23]. A review on the predictions based on Smoluchowski-type theories on the hard sphere system can be found in Jorquera and Dahler's publication [24].

The viscosity of colloidal dispersions contains contributions from the hydrodynamic interaction and the interparticle interaction contribution. The hydrodynamic contribution dominates at low volume fraction. However, at high volume fraction, the interparticle interactions dominate. To some extent, the problem in the polynomial expansions is due to a lack of an accurate description of interactions among the colloidal particles.

We use a systematic method to evaluate the low shear viscosity of interacting suspensions up to high volume fractions. The relative viscosity $\eta_r = \eta/\eta_0$ can be decomposed into the hydrodynamic interaction and the contribution from interparticle interaction,

$$\eta_r = \eta_{\mathrm{HD}} + \eta_I. \tag{18}$$

For calculating the hydrodynamic viscosity of spherical dispersion particles, the Batchelor-Green equation is used [25]:

$$\eta_{\mathrm{HD}} = 1 + 2.5\phi + 5.2\phi^2. \tag{19}$$

The hydrodynamic viscosity is entirely dissipative. The viscoelasticity comes from the contribution of the interparticle interactions. To account for the interaction contribution, Cohen and co-workers investigated the viscoelasticity of the hard sphere system derived from a characteristic cage diffusivity D [26]. Based on earlier theories of Batchelor [21] and Ronis [27], de Schepper, Smorenburg, and Cohen have given a general formula for viscoelasticity in terms of the pair correlation function and the pairwise potential under shear at frequency ω [28]. The interparticle potential can be related to the direct correlation function $c(r)$ under the mean spherical approximation (MSA). The viscoelasticity at zero shear rate has been derived in terms of the equlibrium structure factor $S(k)$ and its derivative $S'(k)$ in momentum space as [28]

$$\eta_I(\phi,\omega) = \frac{k_B T}{60\pi^2\eta_0}\int_0^\infty dk k^4 \left[\frac{S'(k)}{S(k)}\right]^2 \frac{1}{2\omega_H(k) - i\omega}, \tag{20}$$

where

$$\omega_H(k) = \frac{D_0 k^2}{\chi S(k) d(k)} \tag{21}$$

is the linewidth of the dynamic structure factor $S(k,\omega)$ and $d(k) = 1 - j_0(k\sigma) + 2j_2(k\sigma)$, where $j_i(x)$ is the spherical Bessel function of the ith order. Here

$$D_0 = \frac{k_B T}{3\eta_0\pi\sigma} \tag{22}$$

is the Stokes-Einstein diffusivity with σ the diameter of the particle and χ the value of pair correlation function at contact.

The real and imaginary parts of the frequency-dependent complex viscosity $\eta(\omega) = \eta'(\omega) + i\eta''(\omega)$ can be calculated. The viscoelasticity and thus the shear modulus of an interacting system can be theoretically evaluated once the structure factor $S(Q)$ and pair correlation function $g(r)$ are given.

The relative viscosity at zero frequency ω due to the interparticle interaction is given by a numerical integral in Q space ($Q \equiv k\sigma$):

$$\eta_I = \frac{\chi}{40\pi}\int_0^\infty dQ Q^2 d(Q) \frac{[S'(Q)]^2}{S(Q)}. \tag{23}$$

This general formula is quite simple and elegant. The low shear viscosity can be evaluated once an analytical form of the interparticle structure factor $S(Q)$ is known. Analogous to the hydrodynamic interaction, the viscosity due to the interparticle interactions among the solute particles depends on the volume fraction. The integral shows that $S(Q)$ near its peak position has little contribution to the viscosity, contrary to the diffusivity coefficient.

The great advantage of this approach is that the essential quantities in the evaluation of relative viscosity, i.e., volume fraction ϕ and structure factor $S(Q)$, can be obtained from the scattering experiments. This methodology is especially useful when applied to an interacting system for solute concentration above the dilute limit. This method has been used in the hard sphere and charged hard spheres systems. de Schepper, Smorenburg, and Cohen calculated the viscosity and viscoelasticity of the hard spheres up to volume fraction 0.6 [28] and compared with the experimental measurements of silica spheres in cyclohexane [20]. Liu and Sheu modified the formulation and applied to an ionic micellar system with a repulsive interaction in addition to the hard sphere interaction, and extracted the intermicellar structure factor $S(Q)$ from SANS experiments [29].

Previous studies were confined to spherical or quasi-spherical systems with the interparticle interactions of the hard sphere repulsion and ionic repulsion. Here we further extend to systems with an attractive interaction.

We calculate the relative viscosity for a system composed of spherical particles with a hard core and an adhesive surface. The formulation of structure factor $S(Q)$ and its deriva-

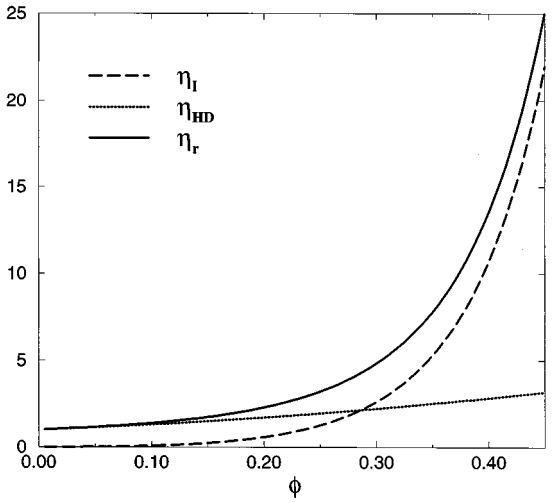

FIG. 7. Relative viscosity η_r for an adhesive hard sphere system as decomposed into contributions from hydrodynamic part η_{HD} (dotted line) and interaction part η_I (dashed line). System parameters are $\Omega=-1$, $\epsilon=0.01$ and $\tau=3.066$. Relative viscosity (solid line) is the sum of the two parts, dominated by η_{HD} at low volume fractions and by η_i at high volume fractions.

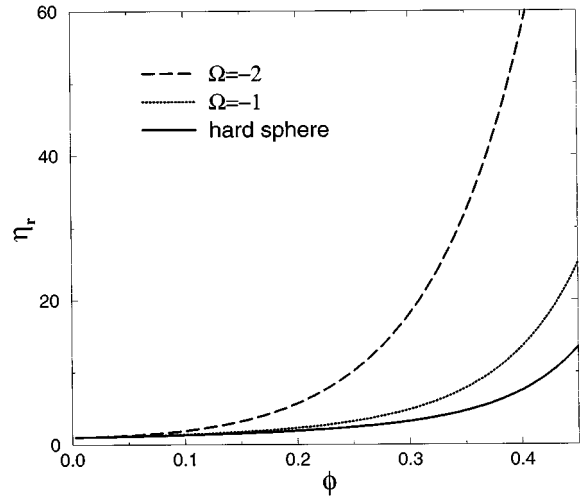

FIG. 8. Theoretical calculation of relative viscosity η_r as a function of volume fraction ϕ for hard sphere (solid line), sticky spheres with surface adhesion potential $\Omega=-1$ (dotted line), and $\Omega=-2$ (dashed line). Surface thickness is fixed at $\epsilon=0.01$.

tive $S'(Q)$ based on Baxter's adhesive hard sphere model was given in Sec. II. The value of the pair correlation function at contact is given by $\chi=\lambda/(12\epsilon)$.

In a simplified sticky sphere model the fractional surface thickness ϵ is taken to be zero for calculating $S(Q)$ [30]. This simplification causes little difference in $S(Q)$ for the Q range considered in small angle neutron and x-ray scattering experiments. However, the sticky sphere model with this simplification cannot be used to evaluate viscosity because of a divergent pair correlation function.

The low shear viscosity of an adhesive hard sphere system is determined by three parameters: the volume fraction ϕ, the surface adhesive potential Ω, and the dimensionless surface layer thickness ϵ. Volume fraction is the only parameter in evaluating the hydrodynamic part of the viscosity. The total relative viscosity and its two contributions as a function of ϕ are illustrated in Fig. 7 for a sticky sphere system with surface potential $\Omega=-1$ and surface layer $\epsilon=0.01$. In this case when ϕ is higher than 0.27, the interaction part dominates the relative viscosity. The exact coefficient a_2 in the hydrodynamic contribution η_{HD} is insignificant. Numerical use of the Batchelor-Green equation ($a_2=5.2$) or the Batchelor equation ($a_2=6.2$) makes a negligible difference in the total relative viscosity.

The surface potential Ω plays a major role in evaluating the low shear viscosity. Figure 8 shows the relative viscosity as a function of ϕ for two surface potential values in comparison with the hard sphere model. It is clear that the surface adhesion increases the relative viscosities significantly. The hydrodynamic contribution η_{HD} is the same, but the interaction contribution η_I for an adhesive hard sphere system starts to dominate at lower ϕ than in the case of the hard sphere system. The attraction can induce phase transition, and its dependence on volume fraction has been discussed in Baxter's original paper [17].

The surface layer thickness ϵ also plays a remarkable role. The effect of layer thickness is significant when the surface potential is very attractive. Figure 9 shows the interaction part of the relative viscosity η_I as a function of surface potential Ω at different ϵ values. Unlike the scattering properties, the rheological behaviors of the adhesive hard sphere systems rely on both surface potential and surface thickness. The second virial coefficient or stickiness parameter $1/\tau$ alone is insufficient for evaluating the low shear viscoelasticity. Although different sets of (Ω,ϵ) may correspond to similar $S(Q)$ at low Q, the discrepancies at large Q (see Fig. 5) are responsible for the different viscosity values. The dependence on large Q can be well understood from the prefactor Q^2 in the numerical integral. Take the same three (Ω,ϵ) sets in Fig. 5, for example. The volume fraction is 0.2 and τ is 3.066 for all three cases. However, the calculated relative viscosity values for the configurations of (0.0986, 0.03), (−1.0, 0.01), and (−2.609, 0.002) are 1.84, 2.28 and 9.3, respectively.

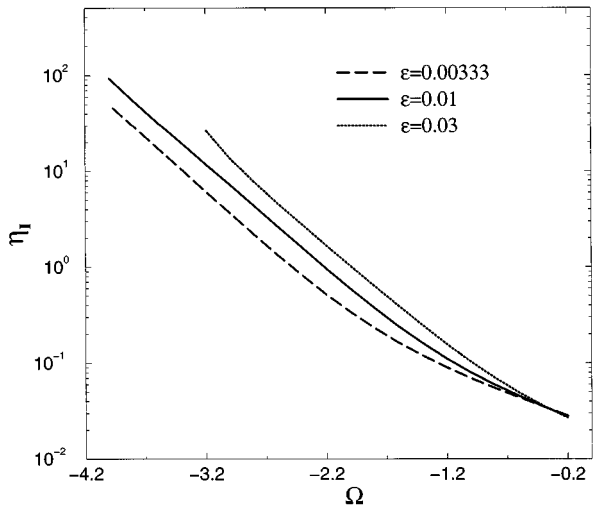

FIG. 9. Contribution from interparticle interaction η_I of the relative viscosity as a function of the surface potential Ω at $\phi=0.1$. Solid, dashed, and dotted lines are for surface thickness $\epsilon=0.003333$, 0.01, and 0.03, respectively.

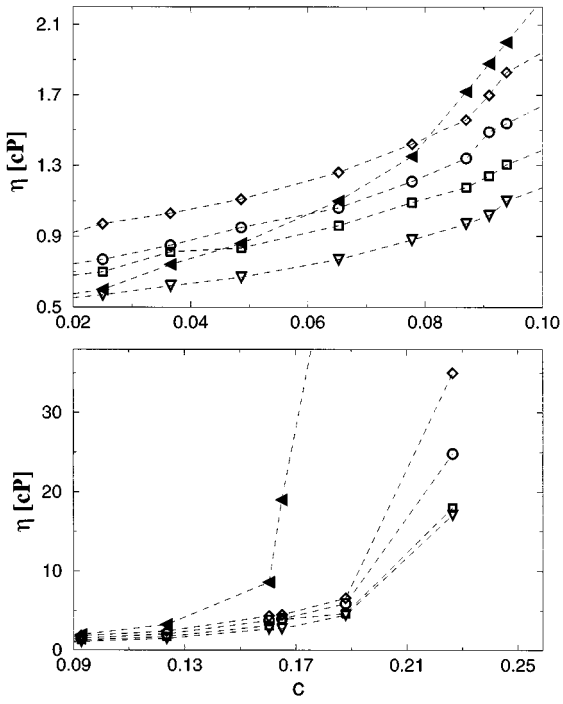

FIG. 10. Measured viscosity η of Pluronic P84 micellar solutions as a function of polymer concentration c (wt %) at various temperatures. The symbols are shown as diamonds (35 °C), circles (40 °C), squares (45 °C), open triangles (55 °C) and filled triangles (60 °). The dashed lines are to guide the eye. Top graph shows the low concentrations and bottom graph shows the higher concentrations.

IV. VISCOSITY OF TRIBLOCK COPOLYMER MICELLES

We develop a method to relate the microstructure to rheological properties of polymeric micellar spheres in aqueous solutions with an attractive intermicellar interaction. The structure-property relationship is of practical importance to many colloidal systems in applications. It links a macroscopic quantity, the solution viscosity, with the microscopic micellar structure on a nanometer scale. In solution, the microscopic information contains not only the details of micellar constitution and structure, but also the specific form and strength of the micelle-micelle interaction. The practicality of this relationship is apparent because both the macroscopic and microscopic quantities can be measured experimentally.

For the polymeric micelles formed by the block copolymer surfactant, the structure and interaction have been successfully obtained from analyses of SANS intensity distribution functions using a model of hard sphere with surface adhesion. To verify the formalism and demonstrate its validity, the theoretical relative viscosity is calculated to compare with experimental measurements.

The viscosity measurements of the Pluronic P84 polymer solutions were made using a Low-Shear30 Contraves Viscometer. Figure 10 shows the measured viscosity as a function of polymer concentration at five temperatures: 35, 40, 45, 55, and 60 °C. The concentration range was chosen the same as in SANS experiments, from 2.6 to 23 wt %. Higher concentrations correspond to the ordered phases and are not studied. The viscosity data at 60 °C differ from those at lower temperatures, indicating the deviation from the spherical shape of the polymeric micelles. The sphere-to-rod transition of micellar solution, i.e., shape effect, has profound influence on rheology. We focus on the spherical particles and analyze viscosity data only in the region of spherical micelles.

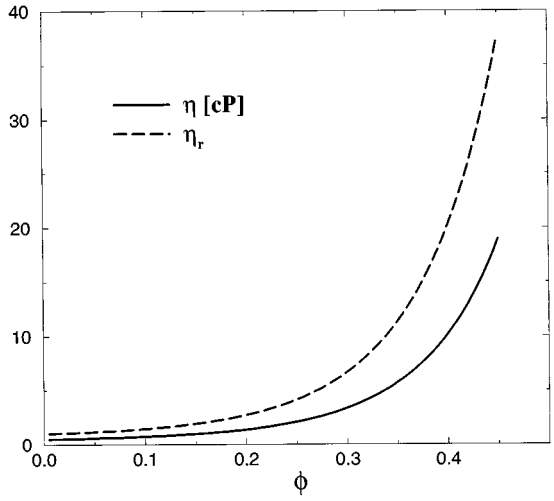

FIG. 11. Theoretical predictions of the viscosity η (units of centipoise) and relative viscosity η_r for triblock copolymer micelles at 55 °C, as a function of hydrated volume fraction ϕ.

Based on the parameters obtained from SANS analyses of the PEO-PPO-PEO micellar solutions, the relative viscosity-volume fraction curves are evaluated using the formulas developed in the previous section. The theoretical values of the viscosity can be calculated by multiplying the solvent viscosity at the corresponding temperature. Figure 11 shows the theoretical curves of the relative viscosity η_r and viscosity η in the unit of centipoise (by multiplying 0.504 cP, the solvent viscosity) as a function of hydrated volume fraction, for the Pluronic P84 micellar solutions at 55 °C.

In the micellar phase, the microstructure of the micelle and the intermicellar interaction potential are highly temperature dependent but independent of the polymer concentration. Upon increasing temperature, the polymeric micelles undergo an increasing tendency of aggregation and dehydration, together with an enhanced surface adhesion. This temperature dependence behavior can be understood from the increasing hydrophobicity of the copolymer surfactant. The microscopic picture of the micelles can also be deduced from the rheological behaviors. In the dilute region careful analysis of intrinsic viscosity can yield the information on the degree of hydration. In the concentrated region viscosity reflects the strength of the intermicellar interactions.

Figure 12 shows the theoretical calculation of the viscosity of triblock copolymer solutions at 35, 40, 45, and 55 °C, in comparison with experimental measurements. The calculations use the volume fraction and potential values extracted from SANS experiments as listed in Table II. It should be noted that no adjustable parameters are used to evaluate η_r at each temperature. The viscosity values at high volume fractions are extremely sensitive to the volume fraction and the surface adhesion. The theoretical curves agree with experimental data very well for all four temperatures. The agreements demonstrate the validity of the assumptions made in the process of formulating the low shear viscosity.

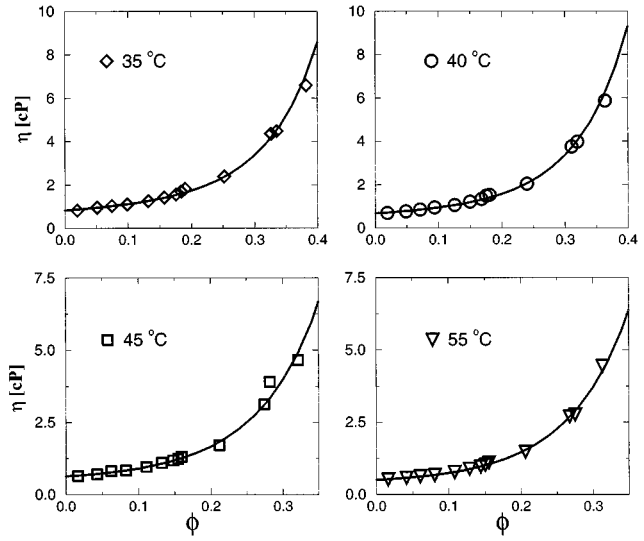

FIG. 12. Theoretical calculations of viscosity (in centipoises) in comparison with experimental measurements at 35, 40, 45, and 55 °C.

V. CONCLUSION

A methodology for studying the relationship between the microstructure and rheology of a nonionic colloidal dispersion with an effective attractive interparticle interaction has been established. As an example, spherical micelles formed by self-association of a triblock copolymer surfactant consisting of polyethylene oxide and polypropylene oxide in aqueous solutions have been investigated at various temperatures and polymer concentrations.

The microstructure of the micelle in nanometer scale is studied in detail with small angle neutron scattering experiments. The aggregation number and hydration number of the micelles are extracted from SANS data analyses. As temperature increases, the aggregation number is enhanced while hydration is suppressed due to the increased hydrophobicity of the block copolymer. At moderate concentrations, the intermicellar interaction is well described by Baxter's potential where a micelle is considered to be a hard sphere with surface adhesion. The attractive interaction at the micellar surface increases with temperature.

Rheology of the polymeric micelles is related to the microstructure and intermicellar interaction in solution. Low shear viscoelasticity is calculated by summing the hydrodynamic interaction and the contribution from the intermicellar interaction. Surface adhesion effectively increases the relative viscosity in comparison with a hard sphere system. The relative viscosity is determined by the surface potential and the surface layer thickness.

The low shear viscosity of the triblock copolymer micelles in aqueous solutions is measured. Theoretical viscosity-volume fraction curves are calculated based on the volume fractions and structure factors extracted from the scattering experiments. Good agreements are obtained up to a volume fraction of 0.4 between the theoretical predictions and the measured values.

The crucial parameters in the evaluation of the low shear viscosity include the volume fraction ϕ, the surface potential Ω, and surface layer thickness ϵ. The micellar volume fraction can be accurately determined by the degree of hydration. The surface potential and adhesive layer thickness describe the short range interactions, and cannot be uniquely determined from SANS alone. On the other hand, viscosity at high concentration is very sensitive to these two parameters. SANS data analysis shows that the effective attraction of the polymeric micelles increases at higher temperature, corresponding to larger $1/\tau$ values. This gives rise to higher relative viscosity. This increase, however, may result either from more negative surface potential Ω or from thicker adhesive layer ϵ. Evaluation of viscosity at high volume fractions allows a more accurate determination of the two parameters.

This methodology, demonstrated in the block copolymer micellar solutions, could be applicable to study the structure-rheology relationship in many polymeric and colloidal systems where the dominant interparticle interaction is attractive.

ACKNOWLEDGMENTS

Y.C.L. is grateful for financial support from Exxon Research and Engineering Company. During the time period in which this research is carried out, the research of SHC is supported by a grant from Materials Science Division of DOE. Thanks go to Dr. D. Schneider and Dr. M.Y. Lin for help with SANS experiments at BNL and NIST. The authors also acknowledge J. C. Sung of Exxon for assistance.

[1] B. Lindman, A. Carlsson, G. Karlstrom, and M. Malmsten, Adv. Colloid Interface Sci. **32**, 183 (1990).

[2] Pluronic and Tetronic Surfactants, Technical Brochure, BASF Corp., Parsipanny, NJ (1989).

[3] P. Alexandridis and T.A. Hatton, Colloids Surf. A **96**, 1 (1995).

[4] Z. Zhou and B. Chu, J. Colloid Interface Sci. **126**, 171 (1988).

[5] W. Brown, K. Schillen, M. Almgren, S. Hvidt, and P. Bahadur, J. Phys. Chem. **95**, 1850 (1991).

[6] K. Mortensen, W. Brown, and B. Norden, Phys. Rev. Lett. **68**, 2340 (1992); K. Mortensen and J. S. Pedersen, Macromolecules **26**, 805 (1993).

[7] P. Alexandridis, J. F. Holzwarth, and T. A. Hatton, Macromolecules **27**, 2414 (1994).

[8] F. Grieser and C. J. Drummond, J. Phys. Chem. **92**, 5580 (1988).

[9] M. Malmsten and B. Lindman, Macromolecules **25**, 5446 (1992).

[10] G. Wanka, H. Hoffmann, and W. Ulbricht, Macromolecules **27**, 4145 (1994).

[11] D. W. Murhammer and C. F. Goochee, Biotechnol. Prog. **6,** 142 (1990).

[12] C. Tanford, *The Hydrophobic Effects: Formation of Micelles and Biological Membranes* (Wiley, New York, 1973).

[13] P. Linse, Macromolecules **27**, 2685 (1994).
[14] G. Karlstrom, J. Phys. Chem. **89**, 4962 (1985); B. Lindman, A. Carlsson, G. Karlstrom, and M. Malmsten, Adv. Colloid Interface Sci. **32**, 183 (1990).
[15] K. Pandya, P. Bahadur, T. N. Nagar, and A. Bahadur, Colloids Surf. **70**, 219 (1993).
[16] J. Hayter and T. Zemb, Chem. Phys. Lett. **93,** 91 (1982); E. Y. Sheu, J. Phys. Chem. **92**, 4466 (1988); Y. C. Liu, P. Baglioni, J. Teixeira, and S. H. Chen, *ibid*. **98**, 10 208 (1994).
[17] R. J. Baxter, J. Chem. Phys. **49**, 2770 (1968); **52**, 4559 (1970).
[18] C. Y. Ku, S. H. Chen, J. Rouch, and P. Tartaglia, Int. J. Thermophys. **16**, 1119 (1995).
[19] A. Einstein, Ann. Phys. (Leipzig) **19**, 289 (1906); **34**, 6917 (1911).
[20] C. G. de Kruif, E. M. F. van Iersel, A. Vril, and W. B. Russel, J. Chem. Phys. **83**, 4717 (1985).
[21] G. K. Batchelor, J. Fluid Mech. **83**, 97 (1977).
[22] R. J. Phillips, J. F. Brady, and G. Bossis, Phys. Fluids **31**, 3462 (1988).
[23] J. F. Brady, J. Chem. Phys. **99**, 569 (1993).
[24] H. Jorquera and J. S. Dahler, J. Chem. Phys. **101**, 1392 (1994).
[25] G. K. Batchelor and J. T. Green, J. Fluid Mech. **56**, 401 (1972).
[26] I. M. de Schepper, E. G. D. Cohen, P. N. Pusey, and H. N. W. Lekerkerker, J. Phys. A **1,** 6503 (1989); I. M. de Schepper and E. G. D. Cohen, Phys. Lett. A **150**, 308 (1990).
[27] D. Ronis, Phys. Rev. A **34**, 1472 (1986).
[28] I. M. de Schepper, H. E. Smorenburg, and E. G. D. Cohen, Phys. Rev. Lett. **5,** 2178 (1993).
[29] Y. C. Liu and E. Y. Sheu, Phys. Rev. Lett. **76**, 700 (1996).
[30] B. Barboy, J. Chem. Phys. **61**, 3194 (1974).